Development of Surface Morphology in Multilayered Films Prepared by Layer-by-Layer Deposition Using Poly(acrylic acid) and Hydrophobically Modified Poly(ethylene oxide)

Jinhwa Seo,[†] Jodie L. Lutkenhaus,[‡] Junoh Kim,[†] Paula T. Hammond,*[,‡] and Kookheon Char*[,†]

School of Chemical and Biological Engineering, Seoul National University, Seoul 151-744, Korea, and the Department of Chemical Engineering, Massachusetts Institute of Technology, Cambridge, Massachusetts 02139

Received January 27, 2007; Revised Manuscript Received March 19, 2007

ABSTRACT: We report the fabrication of free-standing multilayered thin films based on the layer-by-layer (LbL) deposition method. The isolation of multilayer thin film allows us to characterize the materials properties of such films in great detail. Poly(acrylic acid) (PAA) and hydrophobically modified poly(ethylene oxide) (HM-PEO) multilayer films have been prepared using the LbL method based upon hydrogen-bonding interactions. The LbL film composition and thermal properties were obtained as a function of the number of layer pairs using thermal gravimetric analysis (TGA) as well as differential scanning calorimetry (DSC). Above the critical number of layer pairs, the HM-PEO/PAA multilayer films exhibit complex surface structure owing to the hydrophobic nature of HM-PEO (i.e., micelle formation). The unique surface morphology was studied using optical microscopy and fluorescence microscopy, where pyrene dyes incorporated into the hydrophobic cores of HM-PEO micelles allowed us to monitor the sites of HM-PEO micelles. We demonstrate that the film morphology can be controlled by varying the solvent polarity, temperature, and molecular weight of HM-PEO. It is also noted that the introduction of hydrophobic moieties in PEO significantly facilitates the film isolation from various substrates, yielding free-standing multilayer films.

Introduction

The layer-by-layer (LbL) assembly technique is a simple and elegant method to prepare thin and versatile multilayered films and composites based upon noncovalent intermolecular interactions among charged[1,2] or hydrogen-bonding moieties[3,4] (e.g., polyelectrolytes, DNA, proteins, clays, and nanoparticles). First described by Decher et al.,[1,2] numerous and diverse applications such as chemical and biological sensors,[5−7] drug delivery systems,[8−10] photovoltaics[11−13] and electrochromic devices,[14−16] and polymer membranes and electrolytes[17−21] have been achieved. These thin and highly tunable platforms can be precisely controlled to realize optimized material properties (e.g., permselectivity, stability, and conductivity) and other key characteristics for efficient device performance.

Recently, proton-exchange membranes (PEMs) assembled using the LbL technique have demonstrated the promising proton conductivity ($\sim 5.5 \times 10^{-5}$ S/cm) at 100% relative humidity and 25 °C; these thin PEMs were based upon the alternate adsorption of hydrogen-bonding poly(ethylene oxide) (PEO) and poly(acrylic acid) (PAA).[19,20] In present work, we introduce hydrophobically modified poly(ethylene oxide) (HM-PEO) instead of pure PEO in order to study the effect of hydrophobic interactions on the HM-PEO/PAA multilayer systems. HM-PEO has been widely used as a viscosity modifier in paint formulation, paper coating, cosmetics, and building products.[22] Specifically, HM-PEO contains a hydrophilic PEO backbone where both chain ends are capped with hydrophobic alkyl chains through urethane linkages. In dilute solution, flowerlike micelles are formed above the critical micelle concentration, and in semidilute solution, individual HM-PEO micelles connect together through hydrophobic interactions to form a temporary network structure.[23]

While there have been several reports on the LbL assembly of hydrophobically modified[24−27] or amphiphilic polymers,[28−33] only a few studies have shown the influence of hydrophobic domains on the multilayer films. In present study, the effect of hydrophobic moieties (i.e., HM-PEO) on multilayer materials properties was studied in terms of varying solvent polarity, temperature, and polymer molecular weight. Remarkably, large areas of free-standing films were easily obtained because the HM-PEO facilitates weak adsorption between the film and an arbitrary substrate. The morphology of HM-PEO/PAA multilayer films was analyzed using profilometry and optical fluorescence microscopy, and thermal properties of the films were characterized via thermal gravimetric analysis (TGA) as well as differential scanning calorimetry (DSC).

Experimental Section

Materials. Hydrophobically modified poly(ethylene oxide) (HM-PEO), or poly(ethylene oxide) end-capped with alkyl groups using urethane linkages, was synthesized. Details of the synthesis of HM-PEO are described elsewhere.[34−36] Briefly, a PEO chain was end-capped with an alkyl chain of 22 hydrocarbons ends, as shown in Figure 1.

These samples are denoted by HM-PEO35K and HM-PEO20K for hydrophobically modified PEO chains of $M_w = 35\,000$ g/mol and $M_w = 20\,000$ g/mol, respectively. A mixture of PEO (30 g, $M_w = 35\,000$ or 20 000 g/mol, Fluka) and toluene (300 mL) was dried by azeotropic distillation. The mixture was then cooled to 80 °C, and isophorone diisocyanate (Aldrich, three times the number of PEO end groups) was added, followed by the addition of dibutyltin dilaurate (Aldrich, 1−5% of the number of PEO end

* Corresponding authors. E-mail: khchar@plaza.snu.ac.kr; hammond@mit.edu.
[†] Seoul National University.
[‡] Massachusetts Institute of Technology.

10.1021/ma070232j CCC: $37.00
Published on Web 04/28/2007

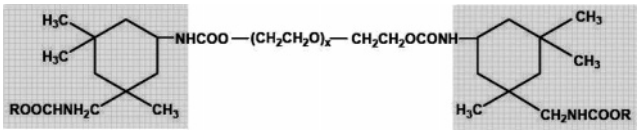

Figure 1. Chemical structure of HM-PEO (R = hydrophobic alkyl chain) used in the present study.

groups). The reaction mixture was kept at 80 °C for 3 h. 1-Docosanol (Aldrich, three times the number of PEO end groups) was added and then mixed until the isocyanate band (2250−2300 cm^{-1}) was no longer observed via FT-IR. Diethyl ether was added to the polymer solution, and the resulting polymer precipitate was dried.

Poly(acrylic acid) (PAA, M_w = 90 000 g/mol) and pyrene were purchased from Polysciences Inc. and used as received.

Silicon wafer, Teflon, polypropylene (PP), poly(dimethylsiloxane) (PDMS), and indium−tin oxide (ITO) were used as substrates for the LbL deposition. Prior to the multilayer film assembly, the substrates were cleaned. Silicon was cleaned under oxygen plasma (100 W, 0.1−0.5 Torr, 5 min). Teflon and PP substrates (VWR) were sonicated in Milli-Q water for 15 min prior to the film deposition. PDMS silicone elastomer kit was obtained from SYLGARD and was used as made. ITO was purchased from Donelly Applied Films and patterned by DCI Inc. to form multiple ITO stripes. The ITO substrates were cleaned by sonication in dichloromethane, acetone, methanol, and Milli-Q water for 15 min.

Dip-Assembled Polyelectrolyte Multilayer Films. All polymer solutions were made by dissolving the polymer in 18 MΩ Milli-Q water. Polyelectrolyte concentrations were 0.02 M based on the repeat unit (alkyl chains of HM-PEO are neglected in calculating the concentration of polymer solutions). The concentration is much higher than the cmc of HM-PEO.[37] All HM-PEO chains in aqueous solution form micelles. HCl and NaOH were used for pH adjustment. Films were prepared with a Carl Zeiss DS50 programmable slide stainer. Substrates were first exposed to HM-PEO solution for 15 min and then rinsed in three baths of Milli-Q water for 2, 1, and 1 min. HM-PEO coated substrates were then dipped into the PAA solution following the same procedure. All the baths were maintained at pH 2.5 in order to suppress the ionization of PAA. These steps comprise one cycle, or "layer pair", and can be repeated for multiple cycles. The nomenclature $(HM\text{-}PEO/PAA)_n$ will be used to denote a multilayer film of n layer pairs of HM-PEO and PAA; when n includes 0.5, HM-PEO is the topmost layer on the surface of the assembled film. To investigate the effect of temperature on the growth and surface properties of the multilayer films, LbL assembly deposition was performed at room temperature (25 °C) and 35 °C. Following assembly, the films were dried under a high-velocity nitrogen stream.

Pyrene dyes were used as an indicator for fluorescence microscopy analysis. In order to guarantee the sufficient infiltration of pyrenes into the hydrophobic cores of micelles, pyrenes were added in the HM-PEO35K solution and stirred for 5 days prior to the multilayer preparation.

Free-standing films were obtained by directly peeling the films off the substrates with tweezers.

Morphology Characterization. Thickness, roughness, and 3D topography of assembled multilayer surfaces were characterized using a Tencor P10 profilometer using a 2 mm stylus tip with 5 mg stylus force. Thickness and surface roughness were measured by scratching the film down to the substrate. The values reported are the average of three or more measurements. Optical and fluorescence images of assembled multilayer films were obtained using a Zeiss Axioplan 2 fluorescence microscope (Carl Zeiss Inc.). Scanning electron microscopy (SEM) images were obtained using a JSM 6060 scanning electron microscope (JEOL Co.). Images of free-standing films were captured with Nikon Coolpix 2500. Dynamic light scattering (DLS) was performed using a BI 9000AT digital autocorrelater (Brookhaven Instruments Corp.) with a 514 nm laser at $\theta = 90^{o}$ at different temperatures (25, 30, and 35 °C) to measure the size of HM-PEO micelles in solution. Data were obtained and analyzed using the Cumulant Fit (CMFT) analysis.

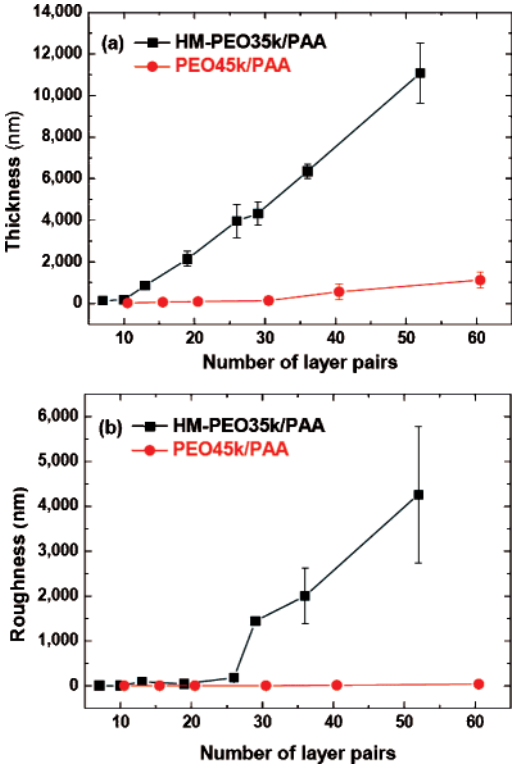

Figure 2. (a) Thickness and (b) roughness growth curve of HM-PEO35K/PAA and PEO45K/PAA multilayer system measured by profilometry.

Thermal Analysis. Free-standing LbL assemblies were characterized using TGA and DSC (TA Instruments Q50 and TA Instruments Q1000, respectively). TGA samples were heated from room temperature to 700 °C at 10 °C/min under nitrogen purge. DSC samples were heated from −90 to 110 °C at a rate of 10 °C/min under nitrogen purge, and the second-scan values were reported. To minimize the effect of humidity, all the samples were dried for 30 min under nitrogen purge prior to thermal measurements.

Results and Discussion

Characteristics of HM-PEO/PAA Multilayer Films. To investigate the effect of hydrophobic alkyl end-chains linked to a PEO chain through urethane linkages, we compare pure PEO/PAA and HM-PEO/PAA multilayer systems of similar molecular weights. Figure 2 shows the thickness and the roughness growth curve of both HM-PEO35K/PAA and PEO45K/PAA multilayer films. Both systems show the linear growth in film thickness (Figure 2a); the thickness of an HM-PEO35K/PAA layer pair (2100 Å) was nearly 8 times larger than the value obtained for pure PEO45K/PAA multilayer films (270 Å/layer pair). Another striking feature of the growth profile is that the surface roughness suddenly increases above a critical number of layer pairs for HM-PEO35K/PAA (Figure 2b). Above 26 layer pairs, the roughness of an HM-PEO35K/PAA multilayer film increases from tens of nanometers to several microns. In contrast, the roughness of a PEO45K/PAA multilayer film remains relatively constant (5−30 nm).

The observed layer pair film thickness of the HM-PEO35K/PAA multilayer films is much higher than other traditional hydrogen-bonding multilayers.[3,38] This phenomenon may be explained by the conformation of HM-PEO within the assembly solution; HM-PEO35K chains form a globular micellar structure where they are subsequently adsorbed to the multilayer surface

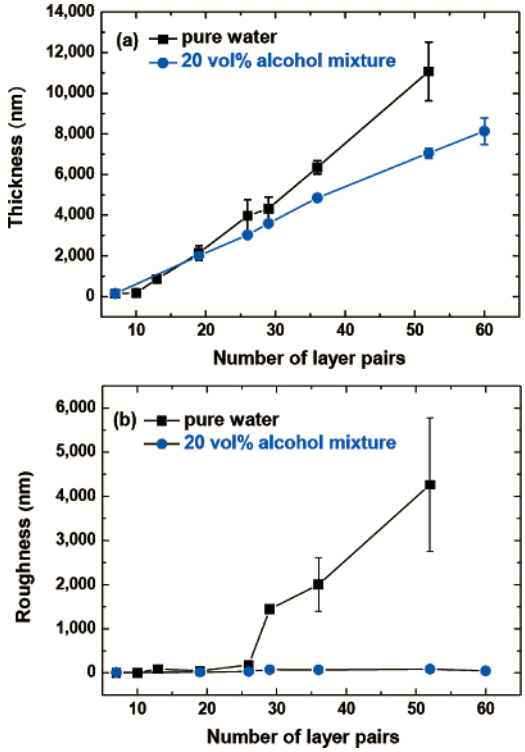

Figure 3. (a) Thickness and (b) roughness growth curve of HM-PEO35K/PAA in pure water solution and in 20 vol % EtOH alcohol mixture solution measured by profilometry.

as micellar aggregates. Evidence of this proposed phenomenon was investigated using fluorescence microscopy and dynamic light scattering, discussed in the following section. Such globular HM-PEO micelles interact with surface-adsorbed PAA chains, causing a loose surface structure; thus, a larger layer pair thickness as well as a larger surface roughness forms relative to the unmodified PEO/PAA multilayer films. We believe that the sharp increase in the film roughness at 26 layer pairs is caused by the grain formation on the multilayer surface owing to the massive aggregation of HM-PEO35K micelles within the film. The origin of the surface structure is not yet clear, but it appears that the concentration of HM-PEO micelles within the film increases during the film assembly through the internal diffusion of HM-PEO, which causes the percolative aggregation of HM-PEO micelles.[23] A detailed study on the diffusion of such micelles within the film is currently in progress.

In order to verify that the large difference in layer pair thickness and surface roughness between pure PEO/PAA and HM-PEO/PAA multilayer films is caused by the formation and aggregation of micelles, we also prepared HM-PEO/PAA multilayer films with a solvent mixture containing 20 vol % ethanol in water, which lowers the polarity (or dielectric constant) of the dipping solution.[39,40] Figure 3 represents the effect of solvent on both thickness and surface roughness of the HM-PEO/PAA multilayer films. Linear LbL growth curves are again obtained for both solvent systems. In the water/alcohol mixture, however, it is noted that the thickness of an HM-PEO35K/PAA layer pair is 1360 Å, which is less than the observed value of the pure water system (2100 Å). A more significant difference can be found in the surface roughness growth profile, as shown in Figure 3b. The sharp increase in the roughness for HM-PEO35K/PAA multilayer films above a certain number of layer pairs in pure water disappears in the water/alcohol mixed solvent. We believe that this originates from the disruption of the HM-PEO35K micellar structure or the complete suppression of the aggregation of micelles in the water/alcohol mixture owing to the suppressed hydrophobic attraction among alkyl chains in less polar medium.

Morphology of HM-PEO/PAA Multilayer Films. The LbL-assembled HM-PEO/PAA multilayer films yield unique film morphology owing to the formation of HM-PEO micelles in pure water. Figure 4 shows the comparison of morphologies of HM-PEO/PAA multilayer films prepared from pure water and from a water/alcohol mixture. The size and height of the surface grains were too large to measure by AFM, so 3D profilometry and optical microscopy were employed to investigate the surface structure. Up to 26 layer pairs, the morphologies of HM-PEO35K/PAA multilayer films in those two systems appear similar, but significant morphological differences are noted above 29 layer pairs. In the water-based system, we clearly observe large grains on the surface of HM-PEO35K/PAA multilayer films. The surface grain size and roughness continue to grow with the number of layer pairs. In contrast, we do not observe any large surface grain structure formation for the HM-PEO35K/PAA multilayer films prepared in the water/alcohol mixture.

Optical microscopy and 3D profilometry clearly demonstrate that the HM-PEO/PAA multilayer films have a unique surface morphology that forms during the LbL assembly process, originating from the hydrophobic attraction among alkyl chains of HM-PEO in aqueous environment. We thus investigated additional parameters to tune the surface morphology of HM-PEO/PAA multilayer films. More specifically, the effect of dipping temperature and of HM-PEO molecular weight was investigated.

To assess the effect of dipping temperature on the surface morphology, HM-PEO35K/PAA multilayer films were prepared at two temperatures (i.e., 25 and 35 °C). The surface morphologies were characterized using optical microscopy, as shown in Figure 5. The surface grain size of HM-PEO35K/PAA multilayer films prepared at 35 °C is much larger than the samples prepared at 25 °C (65 and 20 μm for 30.5 layer pairs in Figure 5, d and b, respectively), and the layer pair thickness doubles when prepared at higher dipping temperature (2100 Å/layer pair at 25 °C vs 4000 Å/layer pair at 35 °C). One possible explanation for this phenomenon could be that HM-PEO micelles in solution increase in size with increasing temperature. To obtain information on the micelle size in solution as a function of temperature, dynamic light scattering (DLS) measurements were performed at 25, 30, and 35 °C and the micellar diameters of HM-PEO were estimated to be 89, 95.3, and 99.3 nm, respectively.

Although the micelle size in solution increases with higher temperature, the difference in micelle size cannot solely explain the large difference in the grain size shown in Figure 5. We believe that several other factors could also contribute to the surface morphology observed at different temperatures. For example, the alkyl chain conformation changes at 35 °C from trans to gauche form which perhaps facilitates the connection between neighboring HM-PEO micelles on the multilayer surface.[41] It is also known that the strength of hydrophobic attraction increases with higher temperature owing to entropic contributions.[42] Conversely, the hydrogen bond energy between PEO and PAA decreases with increasing temperature so that the mobility of HM-PEO chains within the film increases.[43]

Besides varying the deposition temperature, we also have used HM-PEO20K (instead of HM-PEO35K) to assess the effect of PEO molecular weight on the surface morphology of the multilayer films. The surface grains of HM-PEO20K/PAA multilayer films are not quite as remarkable as in the case of

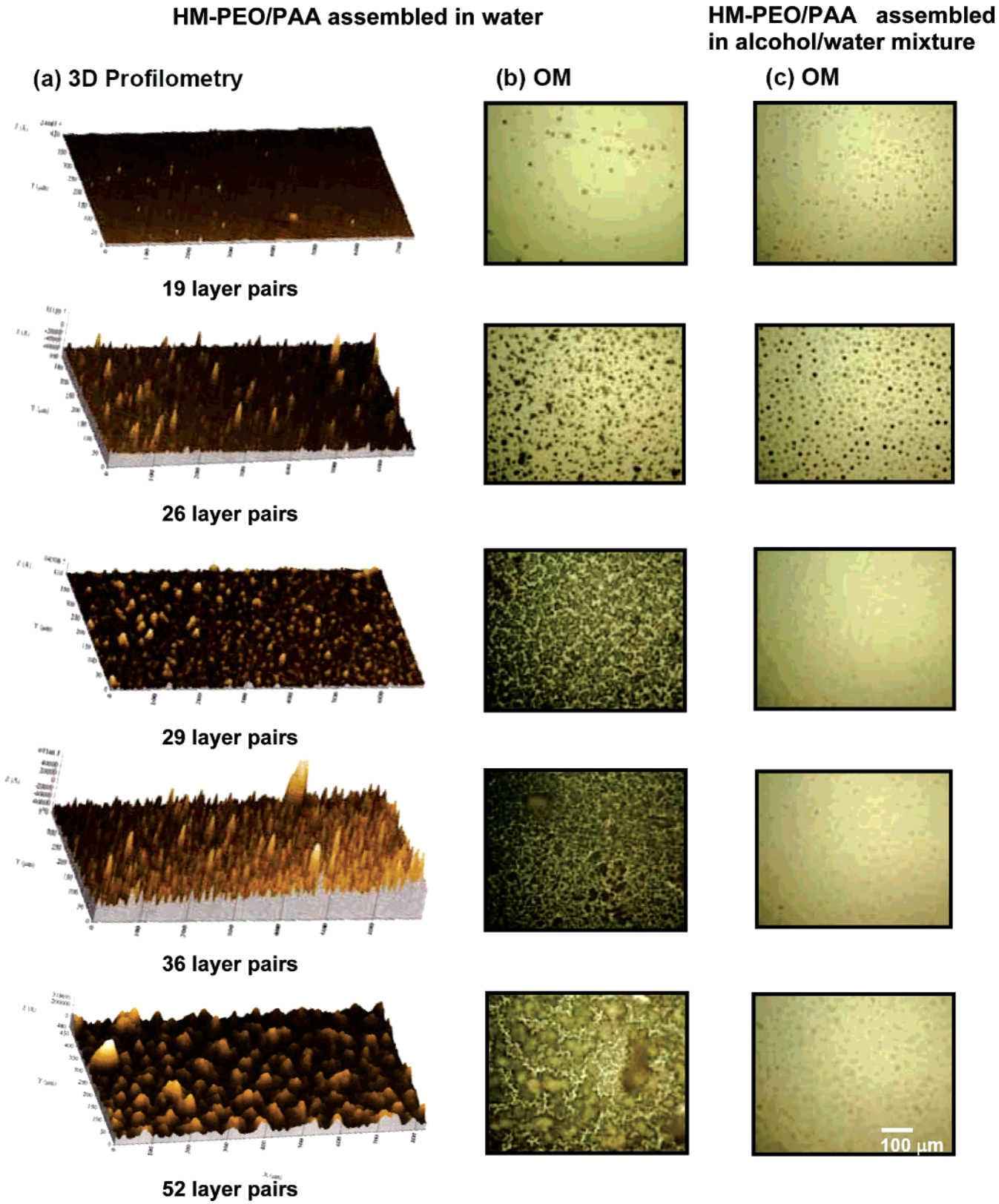

Figure 4. Surface morphology of HM-PEO35K/PAA assembled in pure water (a, b) and 20 vol % EtOH alcohol/water mixture (c) as observed by optical microscopy (OM) and 3D profilometry. The 100 μm scale bar applies to all OM images.

HM-PEO35K/PAA multilayer films, even at increased dipping temperature (Figure 5e,f). In particular, only small and densely populated gains appear on the surface of the $(HM\text{-}PEO20K/PAA)_{30.5}$ multilayer film. The size of HM-PEO20K micelles in solution was also obtained by DLS. The micelle diameter of HM-PEO20K in aqueous solution was found to be 34.4, 36.1, and 40.9 nm at 25, 30, and 35 °C, respectively. These values were almost the half the size of HM-PEO35K in solution.

Because HM-PEO20K has a shorter PEO segment than HM-PEO35K, it is expected that HM-PEO20K micelles are restricted in flexibility and less likely to bridge with neighboring micelles on the multilayer surface, which may explain the difference in

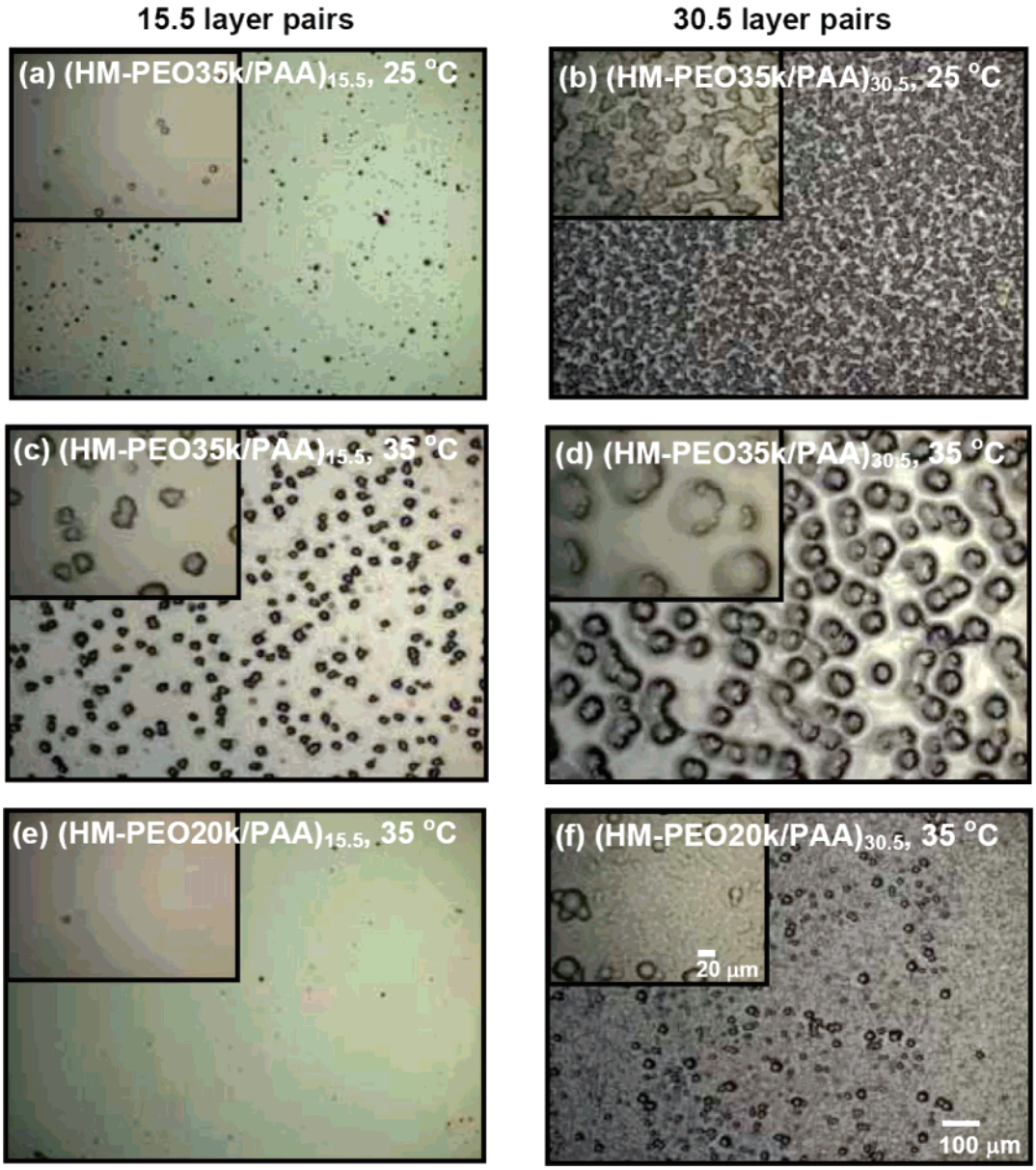

Figure 5. Optical microscopy images of (a) $(HM\text{-}PEO35K/PAA)_{15.5}$ assembled at 25 °C, (b) $(HM\text{-}PEO35K/PAA)_{30.5}$ assembled at 25 °C, (c) $(HM\text{-}PEO35K/PAA)_{15.5}$ assembled at 35 °C, and (d) $(HM\text{-}PEO35K/PAA)_{30.5}$ assembled at 35 °C. Images (e) and (f) are optical microscopy images of $(HM\text{-}PEO20K/PAA)_{15.5}$ and $(HM\text{-}PEO20K/PAA)_{30.5}$ assembled at 35 °C, respectively. Scale bars shown in (f) apply to all images.

surface morphology between the two systems.[44] The layer pair thickness of HM-PEO20K/PAA multilayer film is 1600 and 2200 Å/layer pair at room temperature and 35 °C, respectively. These lower thickness values compared with the values for the HM-PEO35K/PAA multilayer films are reasonable considering the smaller micelle size, as verified by DLS, and the lower chance to form bridges with neighboring micelles in the case of using HM-PEO20K.

As mentioned earlier, the HM-PEO micelles in semidilute solution are known to connect and form a network structure.[23] We thus believe that the observed grain formation on the surface of HM-PEO/PAA multilayer films was attributed to the networking or aggregation of HM-PEO micelles. To demonstrate that the grains on the surface of HM-PEO/PAA multilayer films are caused by the aggregation of HM-PEO micelles, we analyzed HM-PEO35K/PAA multilayer films using fluorescence microscopy. Pyrene dyes were used to monitor the site of HM-PEO micelles; pyrenes are hydrophobic and are selectively encapsulated within the cores of HM-PEO micelles.[45] Figure 6 represents optical and fluorescence microscopy images of HM-PEO35K/PAA multilayer films. Green fluorescence was observed in grain sites on the surface, implying that the grains were composed of HM-PEO micellar aggregates.

Top-down and cross-sectional images of the HM-PEO/PAA multilayer films were taken by SEM. The individual grain formation on the surface of $(HM\text{-}PEO/PAA)_{30}$ is shown in Figure 7a,b. However, the surface morphology of $(HM\text{-}PEO/PAA)_{60}$ appears continuously bumpy and has small grains along the larger bumpy structures (Figure 7c,d). One explanation for the difference in surface morphology observed using SEM is that the concentration of HM-PEO (or HM-PEO micellar aggregate) within the multilayer film increases as the assembly proceeds, discussed in the following section.

Free-Standing HM-PEO/PAA Films. Free-standing multilayer films are of great interest for use as conformable, thin, lightweight, highly sensitive sensing devices[46] and as proton exchange membranes.[20,47] The most popular approach for obtaining free-standing multilayer films is to employ a sacrificial layer consisting of pH-sensitive[48] or soluble polymers such as cellulose acetate (CA).[49,50] Recently, free-standing PEO/PAA

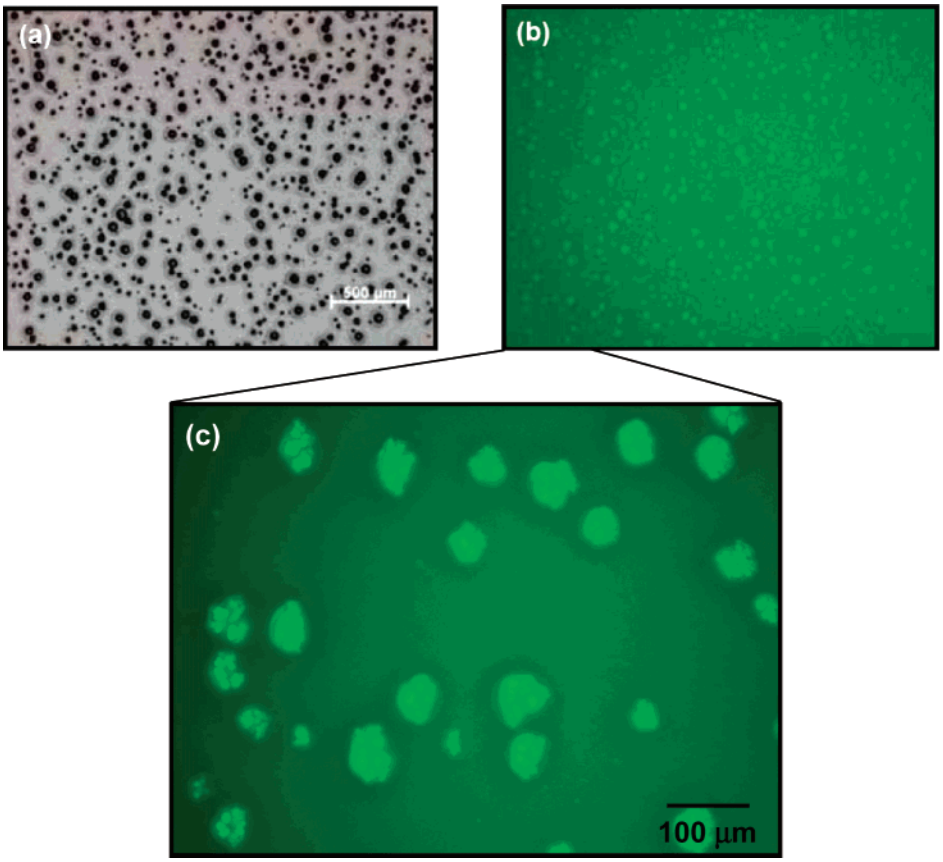

Figure 6. An optical microscopy image (a) and a fluorescence microscopy image (b) of an HM-PEO35K/PAA multilayer film (both images are obtained from the same multilayer film site; scale bar is the same). Image (c) is a magnified image of (b).

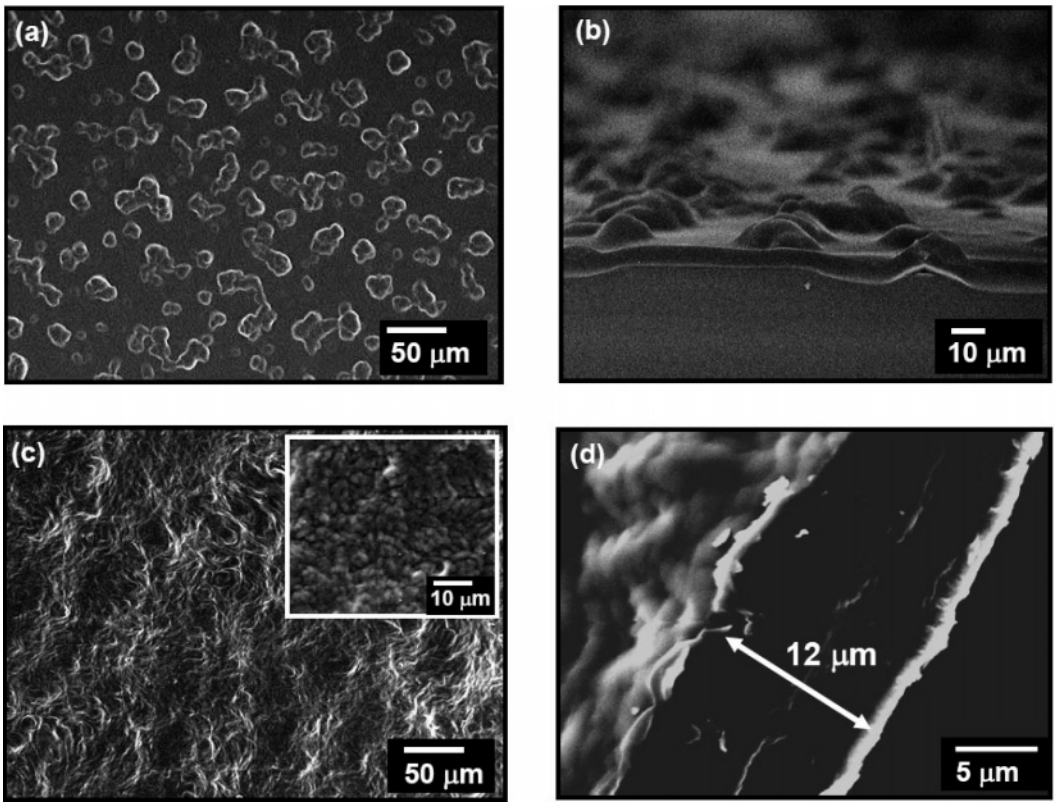

Figure 7. Top-down (a, c) and cross-sectional (b, d) SEM images of an $(HM\text{-}PEO35K/PAA)_{30}$ multilayer film (upper figures) and of an $(HM\text{-}PEO35K/PAA)_{60}$ multilayer film (lower figures).

mulitlayers were obtained without sacrificial layers by the weak adsorption of the multilayer film to a hydrophobic substrate such as Teflon.[47] In comparison, HM-PEO shows even weaker adsorption than PEO against substrates because the micelle formation of HM-PEO in solution causes less contact between the polymers and a substrate, resulting in lower adsorption

Figure 8. Large-area free-standing LbL-assembled (HM-PEO35K/PAA)$_{60}$ multilayer film.

amount at the substrate compared with the adsorption from single molecule solutions of the polymer.[51,52] This difference in multilayer−substrate interactions allows us to obtain free-standing films of HM-PEO/PAA from any type of substrate (i.e., Teflon, polypropylene, PDMS sheets, silicon wafer, or ITO-coated glass). Using the LbL assembly method, which has no sample size restriction, large areas of HM-PEO/PAA free-standing multilayer films were easily prepared. Figure 8 shows a free-standing film of (HM-PEO35K/PAA)$_{60}$, which is 121.4 mm in width, 36 mm in height, and 12 μm in thickness.

The thermal properties of free-standing films were characterized by DSC (Figure 9a) as well as TGA (Figure 9b). Pure HM-PEO exhibits a melting peak at ~60 °C, but in a multilayer film of HM-PEO/PAA, this melting peak was not observed. In other words, the crystallization of HM-PEO was completely suppressed during the multilayer film formation. Additionally, a single glass transition temperature was detected via DSC, indicating some degree of blending and mixing between HM-PEO and PAA within the multilayer structure. In previous work,[47] multilayer films of pure PEO/PAA exhibited a single glass transition temperature (T_g = 35 °C at assembly pH 2.5) as well as suppressed crystallization of pure PEO. Favorable interactions between hydrogen-donor PAA, as well as poly(methacrylic acid), and hydrogen-acceptor PEO have also been described for the case of multilayer films[4,53] and solution-cast interpolymer complexes.[54] The composition within the HM-PEO/PAA multilayer films was determined by the Fox equation:[55]

$$\frac{1}{T_g} = \frac{w_1}{T_{g1}} + \frac{1 - w_1}{T_{g2}}$$

where w_1 is the weight fraction of HM-PEO, T_{g1} is the observed glass transition temperature of HM-PEO (−53 °C), and T_{g2} is the glass transition temperature of PAA (101 °C). It is noted that we use the Fox equation as a simple model, though more sophisticated models exist such as the Gordon−Taylor model[56] which includes a semiquantitative parameter, related to the degree of polymer−polymer interaction. Because we confirmed that the composition measured via DSC and the Fox equation is similar (±3 wt %) to the composition obtained using TGA, we continue to use the Fox equation in our analysis.

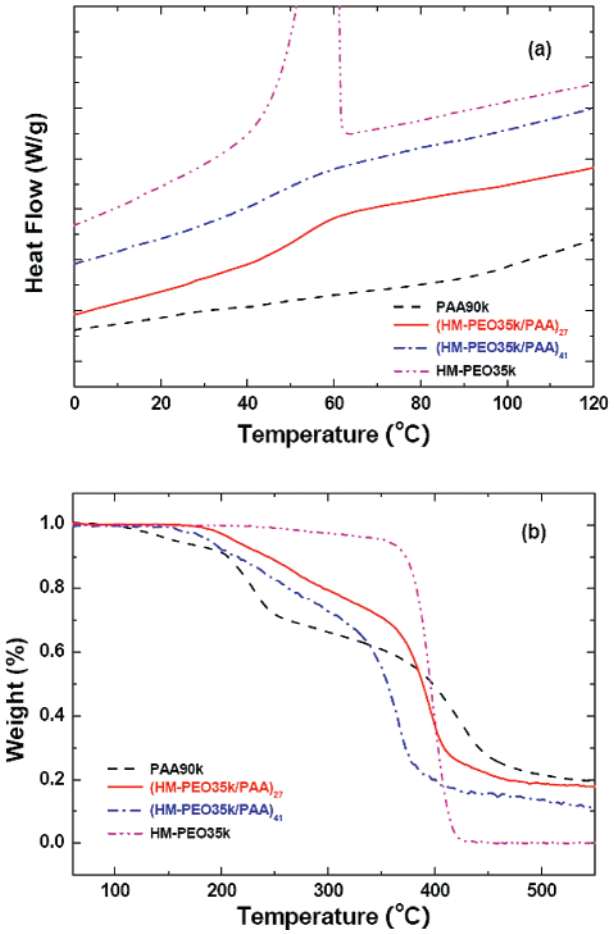

Figure 9. (a) DSC and (b) TGA data of HM-PEO35K/PAA multilayer films, pure HM-PEO, and pure PAA.

Using TGA and DSC, we are able to evaluate the composition of HM-PEO35K/PAA multilayer films as a function of layer pair number (Figures 9 and 10). Interestingly, the weight fraction of HM-PEO within the multilayer film increases as the number of layer pairs is increased. For example, (HM-PEO35K/PAA)$_{27}$ has an HM-PEO weight fraction of 22 or 20 wt % based upon TGA and DSC (T_g = 52.5 °C), respectively; in contrast, (HM-

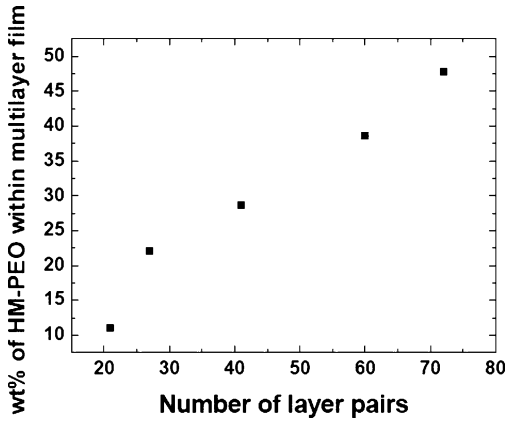

Figure 10. HM-PEO weight fraction within an HM-PEO35K/PAA multilayer film as measured by TGA. HM-PEO fraction increases with the number of layer pairs of an HM-PEO35K/PAA multilayer film.

$PEO35K/PAA)_{41}$ multilayer films have an HM-PEO weight fraction of 28 or 26 wt % based upon TGA and DSC (T_g = 43.3 °C), respectively. For reference, $(PEO/PAA)_{100}$ assembled in analogous conditions gave an PEO weight fraction of 29 wt %, as determined by DSC.[47] The reason why HM-PEO composition in the multilayer films increases with the layer pair number is not yet clear, but lateral or interdiffusion and aggregation of HM-PEO micelles may play a key role.

Conclusions

Multilayer films containing poly(acrylic acid) and hydrophobically modified poly(ethylene oxide), which interact through hydrogen-bonding, have been prepared using the LbL assembly technique. LbL-assembled HM-PEO/PAA multilayer films demonstrate unique surface morphology in comparison with neat PEO/PAA multilayer films owing to the micellar character of HM-PEO in solution. Individual HM-PEO micelles merge or connect through the bridging of HM-PEO chains to form temporary networks along the HM-PEO/PAA multilayer surface, which presents a peculiar surface morphology above the critical number of layer pairs. These films were studied using optical microscopy as well as fluorescence microscopy with pyrene dyes, allowing us to monitor the location of HM-PEO micelles. It is also noted that the film surface morphology can be controlled by varying the solvent polarity. By adding alcohol to an aqueous dipping bath, the solution polarity significantly decreases and the hydrophobic association between alkyl chains is effectively screened, resulting in the suppression of the previously observed surface grain structure. In addition to the solvent effect, the surface structure was also shown to depend upon temperature and molecular weight of PEO segment within the HM-PEO polymer.

Free-standing multilayered HM-PEO/PAA thin films were also obtained, allowing us to characterize composition and thermal properties using TGA and DSC in great detail. It is noted that the introduction of hydrophobic moieties to the multilayer films facilitates film isolation from different types of substrates, yielding large-area free-standing multilayer films. HM-PEO/PAA multilayer films obtained in present study are good candidates for alternative proton exchange membranes in direct methanol fuel cell applications.

Acknowledgment. This work was financially supported by the NANO Systems Institute-National Core Research Center from the Korea Science and Engineering Foundation (KOSEF) and the Brain Korea 21 Program endorsed by the Ministry of Education of Korea. We also acknowledge the Center for Material Science and Engineering and the Institute for the Soldier Nanotechnologies (ISN) at MIT for the use of their facilities. K.C. acknowledges the financial support from the SBS Foundation for his sabbatical leave at ISN of MIT, and J.S. acknowledges the Seoul Science Fellowship.

References and Notes

(1) Decher, G.; Maclennan, J.; Sohling, U.; Reibel, J. *Thin Solid Films* **1992**, *210*, 504.
(2) Decher, G. *Science* **1997**, *277*, 1232.
(3) Stockton, W. B.; Rubner, M. F. *Macromolecules* **1997**, *30*, 2717.
(4) Kharlampieva, E.; Sukhishvili, S. A. *J. Macromol. Sci., Polym. Rev.* **2006**, *46*, 377.
(5) Lvov, Y. M.; Lu, Z.; Schenkman, J. B.; Zu, X.; Rusling, J. F. *J. Am. Chem. Soc.* **1998**, *120*, 4073.
(6) Kim, H.; Doh, J.; Irvine, D. J.; Cohen, R. E.; Hammond, P. T. *Biomacromolecules* **2004**, *5*, 822.
(7) Campas, M.; O' Sullivan, C. *Anal. Lett.* **2003**, *36*, 2551.
(8) Izumrudov, V. A.; Kharlampieva, E.; Sukhishvili, S. A. *Biomacromolecules* **2005**, *6*, 1782.
(9) Berg, M. C.; Zhai, L.; Cohen, R. E.; Rubner, M. F. *Biomacromolecules* **2006**, *7*, 357.
(10) Wood, K. C.; Boedicker, J. Q.; Lynn, D. M.; Hammond, P. T. *Langmuir* **2005**, *21*, 1603.
(11) Mwaura, J. K.; Pinto, M. R.; Witker, D.; Ananthakrishnan, N.; Schanze, K. S.; Reynolds, J. R. *Langmuir* **2005**, *21*, 10119.
(12) Tokuhisa, H.; Hammond, P. T. *Adv. Funct. Mater.* **2003**, *13*, 831.
(13) Man, K. Y. K.; Wong, H. L.; Chan, W. K. *Langmuir* **2006**, *22*, 3368.
(14) Stepp, J.; Schlenoff, J. B. *J. Electrochem. Soc.* **1997**, *144*, L155.
(15) DeLongchamp, D. M.; Kastantin, M.; Hammond, P. T. *Chem. Mater.* **2003**, *15*, 1575.
(16) DeLongchamp, D. M.; Hammond, P. T. *Adv. Funct. Mater.* **2004**, *14*, 224.
(17) Onda, M.; Lvov, Y.; Ariga, K.; Kunitake, T. *J. Ferment. Bioeng.* **1996**, *82*, 502.
(18) DeLongchamp, D. M.; Hammond, P. T. *Chem. Mater.* **2003**, *15*, 1165.
(19) DeLongchamp, D. M.; Hammond, P. T. *Langmuir* **2004**, *20*, 5403.
(20) Farhat, T. R.; Hammond, P. T. *Adv. Funct. Mater.* **2005**, *15*, 945.
(21) Jiang, S. P.; Liu, Z.; Tian, Z. Q. *Adv. Mater.* **2006**, *18*, 1068.
(22) Schaller, E. J.; Sperry, P. R. In *Handbook of Coating Adhesives*; Calbo, L. J., Ed.; Marcel Dekker: New York, 1993; Vol. II, p 105.
(23) Tam, K. C.; Jenkins, R. D.; Winnik, M. A.; Bassett, D. R. *Macromolecules* **1998**, *31*, 4149.
(24) Cochin, D.; Laschewsky, A. *Macromol. Chem. Phys.* **1999**, *200*, 609.
(25) Quinn, J. F.; Caruso, F. *Macromolecules* **2005**, *38*, 3414.
(26) Guyomard, A.; Muller, G.; Glinel, K. *Macromolecules* **2005**, *38*, 5737.
(27) Khopade, A. J.; Mohwald, H. *Adv. Funct. Mater.* **2005**, *15*, 1088.
(28) Emoto, K.; Iijima, M.; Nagasaki, Y.; Kataoka, K. *J. Am. Chem. Soc.* **2000**, *122*, 2653.
(29) Ma, N.; Zhang, H.; Song, B.; Wang, Z.; Zhang, X. *Chem. Mater.* **2005**, *17*, 5065.
(30) Ma, N.; Wang, Y.; Wang, Z.; Zhang, X. *Langmuir* **2006**, *22*, 3906.
(31) Cho, J.; Hong, J.; Char, K.; Caruso, F. *J. Am. Chem. Soc.* **2006**, *128*, 9935.
(32) Qi, B.; Tong, X.; Zhao, Y. *Macromolecules* **2006**, *39*, 5714.
(33) Biggs, S.; Sakai, K.; Addison, T.; Schmid, A.; Armes, S. P.; Vamvakaki, M.; Butun, V.; Webber, G. *Adv. Mater.* **2007**, *19*, 247.
(34) Lundberg, D. J.; Brown, R. G.; Glass, J. E.; Eley, R. R. *Langmuir* **1994**, *10*, 3027.
(35) Vorobyova, O.; Yekta, A.; Winnik, M. A.; Lau, W. *Macromolecules* **1998**, *31*, 8998.
(36) Francois, J.; Maitre, S.; Rawiso, M.; Sarazin, D.; Beinert, G.; Isel, F. *Colloids Surf., A* **1996**, *112*, 251.
(37) Vorobyova, O.; Lau, W.; Winnik, M. A. *Langmuir* **2001**, *17*, 1357.
(38) Sukhishvili, S. A.; Granick, S. *J. Am. Chem. Soc.* **2000**, *122*, 9550.
(39) Dai, S.; Sio, S. T.; Tam, K. C.; Jenkins, R. D. *Macromolecules* **2003**, *36*, 6260.
(40) Char, K.; Frank, C. W.; Gast, A. P.; Tang, W. T. *Macromolecules* **1987**, *20*, 1833.
(41) Lee, Y.; Choi, J.; Choi, Y.; Sohn, D. *J. Phys. Chem. B* **2003**, *107*, 12373.
(42) Koga, K. *J. Chem. Phys.* **2004**, *121*, 7304.
(43) Paeng, K.; Choi, J.; Park, Y.; Sohn, D. *Colloids Surf., A* **2003**, *220*, 1.

(44) Paeng, K. W.; Kim, B.; Kim, E.; Sohn, D. *Bull. Korean Chem. Soc.* **2000**, *21*, 623.
(45) Wang, Y.; Winnik, M. A. *Langmuir* **1990**, *6*, 1437.
(46) Jiang, C.; Tsukruk, V. V. *Adv. Mater.* **2006**, *18*, 1.
(47) Lutkenhaus, J. L.; Hrabak, K. D.; McEnnis, K.; Hammond, P. T. *J. Am. Chem. Soc.* **2005**, *127*, 17228.
(48) Ono, S. S.; Decher, G. *Nano Lett.* **2006**, *6*, 592.
(49) Markutsya, S.; Jiang, C.; Pikus, Y.; Tsukruk, V. V. *Adv. Funct. Mater.* **2005**, *15*, 771.
(50) Tang, Z.; Kotov, N.; Magonov, S.; Ozturk, B. *Nat. Mater.* **2003**, *2*, 413.
(51) Xiao, L.; Xu, G.; Chen, A.; Yuan, S. *Colloids Surf., A* **2003**, *219*, 233.
(52) Stuart, M. A. C.; Fokkink, R. G.; Horst, P. M.; Lichtenbelt, J. W. T. *Colloid Polym. Sci.* **1998**, *276*, 335.
(53) Sukhishvili, S.; Granick, S. *Macromolecules* **2002**, *35*, 301.
(54) Lu, X.; Weiss, R. A. *Macromolecules* **1995**, *28*, 3022.
(55) Fox, T. G. *Bull. Am. Phys. Soc.* **1956**, *1*, 123.
(56) Gordon, M.; Taylor, J. S. *J. Appl. Chem. USSR.* **1952**, *2*, 493.

MA070232J